Chalcogenide Letters Vol. 14, No. 8, August 2017, p. 297 - 302

SURFACE PLASMON RESONANCE SIMULATIONS IN STRUCTURES WITH CHALCOGENIDE LAYER

L. BASCHIR*, A. A. POPESCU, D. SAVASTRU, S. MICLOS
National Institute R&D of Optoelectronics INOE 2000, 409 Atomistilor str., PO BOX MG. 5, RO-077125 Magurele, Ilfov, Romania

The use of amorphous chalcogenide layer in structures using surface plasmon resonance improves the sensitivity of sensors using such structures by providing them with sharp resonance characteristics. Thus very small changes (up to 10^{-6}) of the refractive index cause important changes of the reflectivity. The transfer matrix formalism approach was used to determine reflectances for s- and p-polarizations, for different combinations of thicknesses of metal and chalcogenide layers, over a large wavelength range. 3D maps and statistics tables illustrate the process of plasmonic structure design in order to obtain an optimal sensitivity.

(Received June 12, 2017; Accepted August 7, 2017)

Keywords: Photonics, Plasmonics, Chalcogenide Amorphous Materials, Attenuation coefficient

1. Introduction

Plasmonics is a promising topic, studied from early 20th century, exploring phenomena based on interaction between electromagnetic radiation and conduction electrons at metallic interfaces or in small metallic nanostructures (thus entering in the field of nanophotonics). This interaction shows how electromagnetic fields can be confined over wavelength and sub-wavelength dimensions inside the metallic layer [1-5] and, consequently, to a minimum transmission intensity. An incident p-polarized (transversal magnetic) light beam satisfying the resonance condition generates a wave that may propagate along a thin film at metal-dielectric interface resulting a surface plasmonic wave. The excitation of the surface plasmons in a metal layer is done by using evanescent waves formed by total reflection in a prism configuration (E. Kretschmann and H. Raether [1]). Confinement is obtained when the light is directed on the prism at a resonance angle, on the metal-air (or metal-dielectric) interface and is put in evidence by determining the angle of incidence of the light on the prism at which the resonance appears [1-2,5-6].

An approach is to solve Helmholtz wave equation, derived from Maxwell's equations [7-11]. This approach is effective when complex effective refractive index is required for a given wavelength. The aim of this study is to determine the resonance peaks for different combinations of metal and chalcogenide layers thicknesses over a large wavelength range (405-1625 nm). Therefore the transfer matrix formalism approach was chosen [5,12].

The simulation results should be compared to measurements [13]: first the structure is simulated and best combination of metal and chalcogenide layers thicknesses is found, of course for available laser sources. Once the best combination found, measurements are carried out to determine the exact incidence angle and the reflectance corresponding to the resonance peak.

2. Theoretical considerations

Unlike the Helmholtz wave equation, where models differ with the number of layers (the number of equations differs), the matricial approach is the same for any number of layers.

*Corresponding author: baschirlaurentiu@inoe.ro

Considering N layers, and the next notations: j – layer current number (between 1 and N), n_{pj}, n_{sj} –refractive index of the medium j for p respectively s polarization, k_{pj}, k_{sj} – extinction coefficient of medium j for p respectively s polarization, d_j – thickness of medium j (d_1 and $d_N = 0$, being semi-infinite media), $e_{pj} = (n_{pj} + \mathrm{i}\cdot k_{pj})^2$ – complex refractive index for p polarization, $e_{sj} = (n_{sj} + \mathrm{i}\cdot k_{sj})^2$ – complex refractive index for s polarization, i – incidence angle current number (between 1 and i_{max}), θ_i – incidence angle, the reflectance is calculated for each θ as it follows.

Calculations are done for both p polarization and s polarization. For an easier understanding of subsequent equations, next notations were done:

$$q_{pj} = \frac{\sqrt{e_{pj} - \left(n_{p1}\cdot\sin\theta\right)^2}}{e_{pj}} \qquad q_{sj} = \sqrt{e_{sj} - \left(n_{s1}\cdot\sin\theta\right)^2} \tag{1}$$

$$\beta_{pj} = \left(\frac{2\pi\cdot d_j}{\lambda}\right)\cdot\sqrt{e_{pj} - \left(n_{p1}\cdot\sin\theta\right)^2} \qquad \beta_{sj} = \left(\frac{2\pi\cdot d_j}{\lambda}\right)\cdot\sqrt{e_{sj} - \left(n_{s1}\cdot\sin\theta\right)^2} \tag{2}$$

In the above notations subscript p relates to p polarization, s - to s polarization, while j is the current number of the layer.

Then, for each layer j are calculated the transfer matrices M_{pj} (for p polarization) and M_{sj} (for s polarization):

$$M_{pj} = \begin{bmatrix} \cos\left(\beta_{pj}\right) & -i\cdot\sin\left(\beta_{pj}\right)/q_{pj} \\ -i\cdot\sin\left(\beta_{pj}\right)\cdot q_{pj} & \cos\left(\beta_{pj}\right) \end{bmatrix} \qquad M_{sj} = \begin{bmatrix} \cos\left(\beta_{sj}\right) & -i\cdot\sin\left(\beta_{sj}\right)/q_{sj} \\ -i\cdot\sin\left(\beta_{sj}\right)\cdot q_{sj} & \cos\left(\beta_{sj}\right) \end{bmatrix} \tag{3}$$

Finally are calculated the total transfer matrices T_p (for p polarization) and T_s (for s polarization):

$$T_p = \prod_{j=0}^{N} M_{pj} \qquad T_s = \prod_{j=0}^{N} M_{sj} \qquad \text{where} \quad M_{p0} = M_{s0} = \begin{bmatrix} 1 & 0 \\ 0 & 1 \end{bmatrix} \tag{4}$$

Now, the reflectances R_p (for p polarization) and R_s (for s polarization) are calculated as:

$$R_p = \left| \frac{\left(T_p(0,1)\cdot q_{pN} + T_p(0,0)\right)\cdot q_{p1} - \left(T_p(1,1)\cdot q_{pN} + T_p(1,0)\right)}{\left(T_p(0,1)\cdot q_{pN} + T_p(0,0)\right)\cdot q_{p1} + \left(T_p(1,1)\cdot q_{pN} + T_p(1,0)\right)} \right|$$
$$R_s = \left| \frac{\left(T_s(0,1)\cdot q_{sN} + T_s(0,0)\right)\cdot q_{s1} - \left(T_s(1,1)\cdot q_{sN} + T_s(1,0)\right)}{\left(T_s(0,1)\cdot q_{sN} + T_s(0,0)\right)\cdot q_{s1} + \left(T_s(1,1)\cdot q_{sN} + T_s(1,0)\right)} \right| \quad (5)$$

3. Discussion of the simulation results

Simulation considered several combinations of thicknesses of metal (gold) and dielectric (As_2S_3) layers in a 4-layer structure: GaP (material of the coupling prism) – Au (metal layer) – As_2S_3 (dielectric layer) – Air. There were considered three gold thicknesses (40, 45 and 50 nm) and four As_2S_3 thicknesses (300, 500, 700 and 1000 nm). 3D mappings for R_p and R_s (exemplified in Figs. 1-4) are calculated for 21 wavelengths corresponding to usual laser sources (mostly laser diodes) emitting in the range 405 – 1625 nm and for incidence angles θ ranging between 10° and 80°.

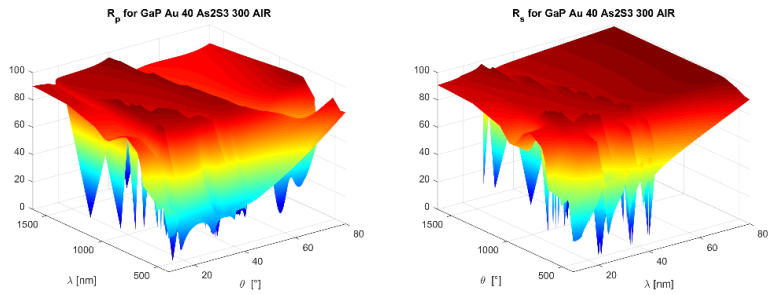

Fig. 1. 3D mapping of R_p and R_s of Au 40 nm and As_2S_3 300 nm thickness

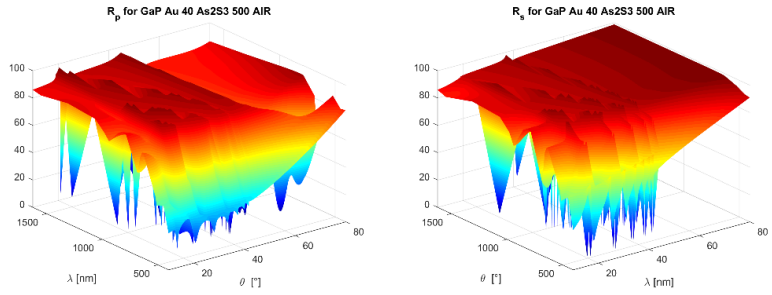

Fig. 2. 3D mapping of R_p and R_s of Au 40 nm and As_2S_3 500 nm thickness

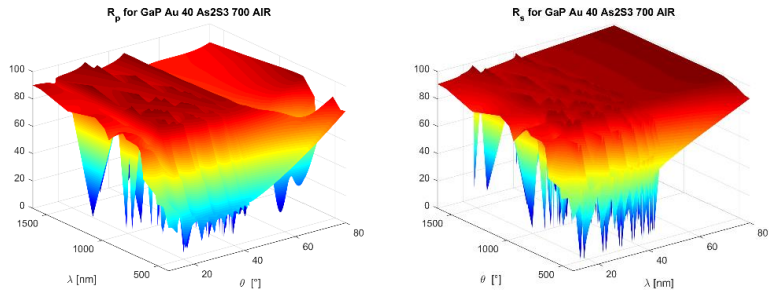

Fig. 3. 3D mapping of R_p and R_s of Au 40 nm and As_2S_3 700 nm thickness

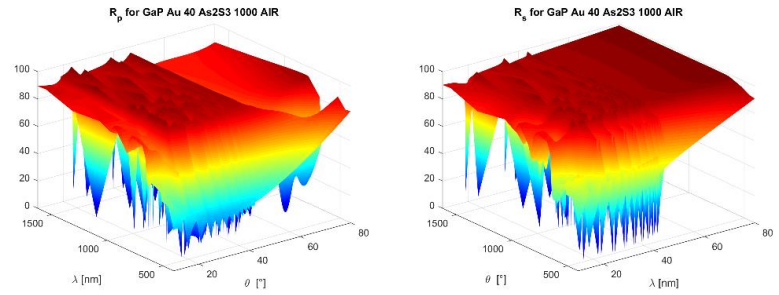

Fig. 4. 3D mapping of R_p and R_s of Au 40 nm and As_2S_3 1000 nm thickness

Only two of the 21 wavelengths were chosen to illustrate the study: 1310 nm and 1550 nm, the two wavelengths used in optical fibre communications. Resulting data are presented in Table 1 and Fig. 5, respectively in Table 2 and Fig. 6.

Table 1. R_p and R_s minima at λ = 1310 nm

λ = 1310 nm	Au 40 nm		Au 45 nm		Au 50 nm	
	R_p	R_s	R_p	R_s	R_p	R_s
As_2S_3 300 nm	0.004	3.15	3.32	11.73	12.79	24.06
As_2S_3 500 nm	0.02	1.43	3.05	8.30	12.36	19.55
As_2S_3 700 nm	0.03	2.88	3.00	11.24	12.28	23.42
As_2S_3 1000 nm	0.01	2.25	2.98	10.06	12.26	21.94

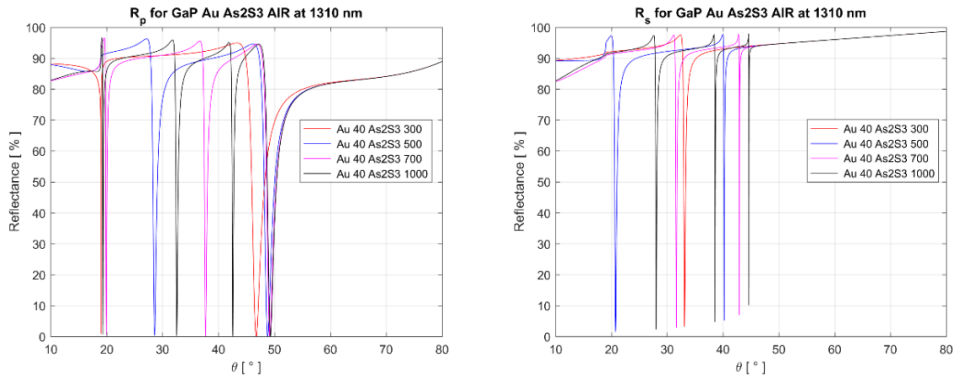

Fig. 5. R_p and R_s at λ = 1310 nm

Table 2. R_p and R_s minima at λ = 1550 nm

λ = 1550 nm	Au 40 nm		Au 45 nm		Au 50 nm	
	R_p	R_s	R_p	R_s	R_p	R_s
As_2S_3 300 nm	1.15	7.74	8.05	18.58	19.61	31.80
As_2S_3 500 nm	0.77	10.72	7.12	22.51	18.42	36.07
As_2S_3 700 nm	0.69	7.00	6.91	17.53	18.13	30.60
As_2S_3 1000 nm	0.66	5.93	6.82	15.99	18.02	28.87

For both wavelengths the best solutions (the lowest R_p and R_s minima) are obtained for the thinnest gold layer (40 nm). Regarding polarization, R_p minima are considerably lower than R_s

minima. At 1310 nm an absolute R_p minimum of 0.004 % was obtained for an As_2S_3 layer of 300 nm while an absolute R_s minimum of 1.43 % was obtained for an As_2S_3 layer of 500 nm.

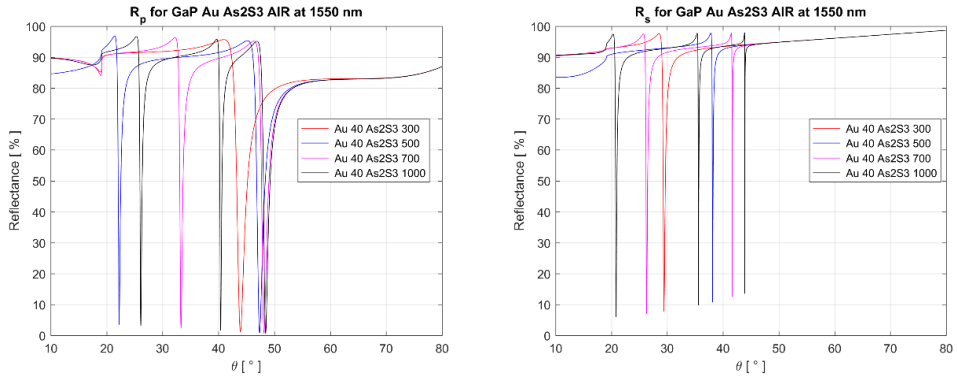

Fig. 6. R_p and R_s at λ = 1550 nm

The highest R_p minimum obtained at 1310 nm was 0.03 % for an As_2S_3 layer of 700 nm.

At 1550 nm the minima are higher: R_p minima from 0.66 % for an As_2S_3 layer of 1000 nm to 1.15 % for an As_2S_3 layer of 300 nm and R_s minima from 5.93 % for an As_2S_3 layer of 1000 nm to 10.72 % for an As_2S_3 layer of 500 nm.

4. Conclusions

Electric and magnetic field distribution within the waveguide regions, propagation constants were calculated and the attenuation of different TE and TM modes necessary for coupling the light into plasmonic waveguide via prism with low refractive index was evaluated. The investigations of the guided modes provided numerical results on plasmonic waveguide structures.

Transfer matrix formalism approach applied to a wide wavelength range (405-1625 nm), that includes the most used laser sources, and to large range of incidence angles (from 10° to 80°, by a very fine step – 0.005°) provides a very useful and powerful tool to design plasmonic waveguide structures.

A certain structure being studied (a gold layer, a chalcogenide GaLaS amorphous film of finite thickness and semi-infinite cover air, in this case) some combinations of layer thicknesses (gold and chalcogenide, in the example) may be evaluated, first analysing the 3D mappings of R_p and R_s and then selecting the wavelengths of interest for the respective application.

Statistics (minimum reflectance value and position for both polarizations) are calculated, as in Table 1 and 2. Summarizing these data for all tested combinations conclusions can be drawn allowing to select the best thickness combination for the respective application. Useful conclusions may be also drawn analysing the influence of the variations of the thickness of a certain layer. For instance, in the studied example, the best results are obtained for the thinnest (40 nm) golden layer and for the thickest (1000 nm) As_2S_3 layer.

Results can be refined by giving tolerances to the optimal found thickness combination in order to find the influences over the amplitude and position of the reflectance minima. This information is very important in the design of a plasmonic sensor.

Acknowledgement

This work was supported by a grant of the Romanian National Authority for Scientific Research, ANCSI, project number PN-16.40.01.01 / 2016.

References

[1] E. Kretschmann, H. Raether, Z. Naturforschung, **23a**, 2135 (1968).
[2] S. A. Maier, Plasmonics – Fundamentals and Applications, Springer, New York, 2007.
[3] R. D. Roy, R. Chattopadhyay, S.K. Bhadra, Photonics Research **1**, 164 (2013).
[4] Z. L. Sámson, S.-C. Yen, K. F. MacDonald, K. Knight, S. Li, D. W. Hewak, D.-P. Tsai, N.I. Zheludev, Phys. Status Solidi RRL **4**, 274 (2010).
[5] A.A. Popescu, R. Savastru, D. Savastru, S. Miclos, Dig. J. Nanomater. and Bios. **6**, 1245 (2011).
[6] H. Raether, Surface Plasmons on Smooth and Rough Surfaces and on Gratings, Springer, Berlin, Germany, 1988.
[7] G. C. Vasile, A. A. Popescu, M. Stafe, S.A. Koziukhin, D. Savastru, S. Donţu, L. Baschir, V. Sava, B. Chiricuţă, M. Mihăilescu, C. Neguţu, N. N. Puşcaş, UPB Sci. Bull. – Ser. A **75**, 311 (2013).
[8] A. A. Popescu, L. Baschir, D. Savastru, M. Stafe, C. Negutu, V. Savu, G. Vasile, M. Mihailescu, V.V. Verlan, O. Bordian, N.N. Puscas, Rom. Rep. Phys. **67**, 1421 (2015).
[9] A. A. Popescu, L. Baschir, D. Savastru, M. Stafe, G. C. Vasile, S. Miclos, C. Neguţu, M. Mihailescu, N.N. Puscas, UPB Sci. Bull. – Ser. A **77**, 233 (2015).
[10] M. Stafe, G. C. Vasile, A. A. Popescu, D. Savastru, L. Baschir, M. Mihailescu, C. Negut, N.N. Puscas, Proc. SPIE **9258**, 92582H-1 (2015).
[11] S. Miclos, D. Savastru, A. Popescu, L. Baschir, R. Savastru, UPB Sci. Bull. – Ser. A **78**, 283 (2016).
[12] G.C. Vasile, R. Savastru, A.A. Popescu, M. Stafe, D. Savastru, S. Dontu, L. Baschir, V. Sava, B. Chiricuta, M. Mihailescu, C. Negutu, N.N. Puscas, Rom. Rep. Phys. **65**, 1012 (2013).
[13] S. Dontu, A.A. Popescu, D. Savastru, V. Sava, B. Chiricuta, M. Mihailescu, C. Negutu, G. Vasile, N.N. Puscas, UPB Sci. Bull. – Ser. A **75**, 163 (2013).